

A Task is Worth One Word: Learning with Task Prompts for High-Quality Versatile Image Inpainting

Junhao Zhuang^{1,2*}Yanhong Zeng²Wenran Liu²Chun Yuan¹ ✉Kai Chen² ✉¹Tsinghua Shenzhen International Graduate School, Tsinghua University²Shanghai AI Laboratory

{zhuangjh23@mails, yuanc@sz}.tsinghua.edu.cn

{zengyanhong, liuwenran, chencai}@pjlab.org.cn

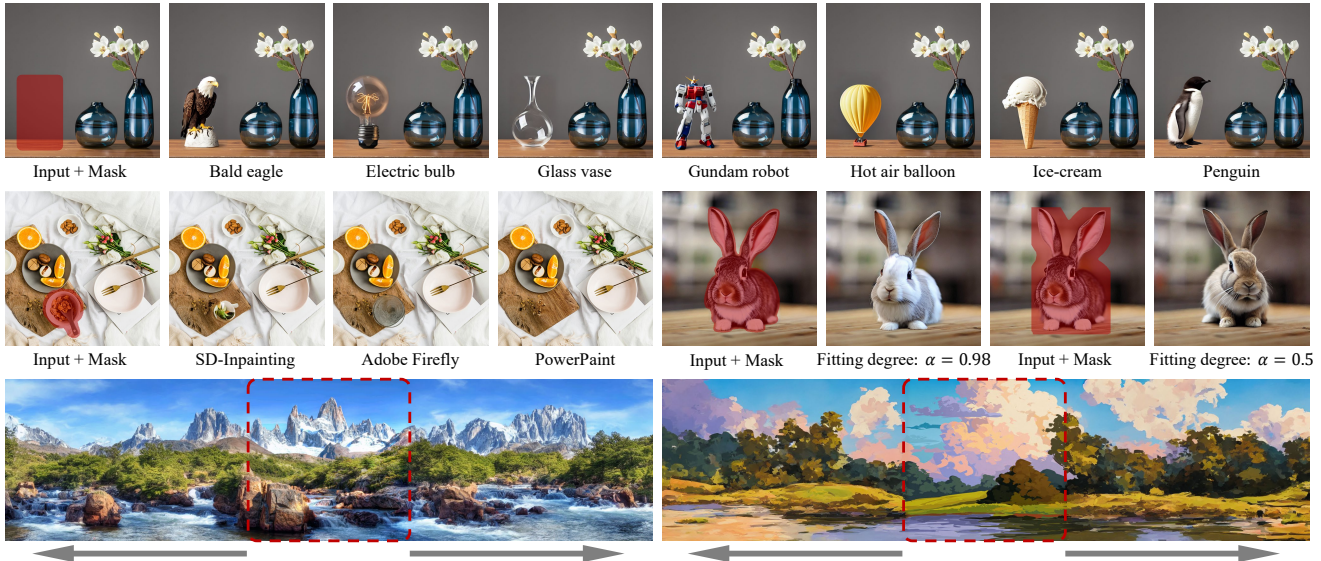


Figure 1. **PowerPaint** is the first versatile image inpainting model that simultaneously achieves state-of-the-art results in various inpainting tasks such as text-guided object inpainting, context-aware image inpainting, shape-guided object inpainting with controllable shape-fitting, and outpainting. [Best viewed in color with zoom-in].

Abstract

Achieving high-quality versatile image inpainting, where user-specified regions are filled with plausible content according to user intent, presents a significant challenge. Existing methods face difficulties in simultaneously addressing context-aware image inpainting and text-guided object inpainting due to the distinct optimal training strategies required. To overcome this challenge, we introduce **PowerPaint**, the first high-quality and versatile inpainting model that excels in both tasks. First, we introduce learnable task prompts along with tailored fine-tuning strategies to guide the model’s focus on different inpainting targets explicitly. This enables **PowerPaint** to accomplish various inpainting tasks by utilizing different task prompts, resulting in state-of-the-art performance. Second, we demonstrate the versa-

tility of the task prompt in **PowerPaint** by showcasing its effectiveness as a negative prompt for object removal. Additionally, we leverage prompt interpolation techniques to enable controllable shape-guided object inpainting. Finally, we extensively evaluate **PowerPaint** on various inpainting benchmarks to demonstrate its superior performance for versatile image inpainting. We release our codes and models on our project page: <https://powerpaint.github.io/>.

1. Introduction

Image inpainting aims to fill in user-specified regions in an image with plausible contents [4]. It has found widespread application in practical domains such as photo restoration [3, 17, 19] and object removal [21, 29, 35]. With the explosive popularity of text-to-image (T2I) models [24, 25, 27, 37], inpainting has become even more crucial, offering a flexible and interactive way to mask unsatisfied regions in generated

* Work done during an internship in Shanghai AI Laboratory.

✉ Corresponding authors.

images and regenerate them for perfect results [31, 32].

Despite the significant practical benefits, achieving high-quality versatile image inpainting remains a challenge [19, 29, 35]. Early inpainting models are usually trained by randomly masking a region in an image and then recovering it [19, 21, 35]. Such a design encourages models to attend to the image context and utilize it for inpainting, yielding promising results. However, these models assume that the missing content can be inferred from the context, making it hard to synthesize novel objects [29, 35]. Recent advancements have seen a shift towards text-guided image inpainting, where a pre-trained T2I model is fine-tuned using masks and text descriptions, resulting in remarkable outcomes in object synthesis [25, 31–33]. However, these approaches introduce a bias that assumes the presence of objects in the masked regions. To remove unwanted objects for a clean background, these models often require extensive prompt engineering or complex workflow. Moreover, these methods remain vulnerable to generating random artifacts that lack coherence with the image context [31, 32].

To address the above limitations, we propose **PowerPaint**, the first high-quality versatile inpainting model capable of both text-guided object inpainting and context-aware image inpainting. The key to achieving different inpainting targets in a single model lies in utilizing distinct learnable task prompts and tailored fine-tuning strategies. First, to fine-tune a T2I model for inpainting, we introduce two learnable prompts, \mathbf{P}_{obj} and \mathbf{P}_{ctxt} , for text-guided object inpainting and context-aware image inpainting, respectively. \mathbf{P}_{obj} is optimized by using object bounding boxes as masks and appending \mathbf{P}_{obj} as a suffix to the text description, while \mathbf{P}_{ctxt} is optimized with random masks and \mathbf{P}_{ctxt} itself as the text prompt. Through such training, \mathbf{P}_{obj} is able to prompt the PowerPaint to synthesize novel objects based on text descriptions, while using \mathbf{P}_{ctxt} can fill in coherent results according to the image context without any additional text hints. Moreover, the learned task prompt in PowerPaint has effectively captured the intrinsic pattern of the task and can be extended to facilitate powerful object removal. In particular, existing T2I models employ a classifier-free guidance sampling strategy, where a negative prompt can effectively suppress undesired effects [8, 12]. By leveraging this sampling strategy and designating \mathbf{P}_{ctxt} as the positive prompt and \mathbf{P}_{obj} as the negative prompt, PowerPaint can effectively prevent the generation of objects in the region and significantly enhance the success rate of object removal [25].

We further demonstrate the ability to achieve a trade-off between two different inpainting tasks through prompt interpolation. To achieve this, we introduce an additional task prompt $\mathbf{P}_{\text{shape}}$, which is trained using object segmentation masks and object descriptions. Generating objects within coarse masks typically encompasses both context-aware background filling and text-based foreground synthe-

sis. Therefore, we establish a trade-off between these two inpainting targets, by randomly dilating the object segmentation masks and using the interpolation between $\mathbf{P}_{\text{shape}}$ and \mathbf{P}_{ctxt} as the task prompt for training. The degree of interpolation is determined by the increased area ratio after mask dilation, providing users with control over how closely the generated objects should align with the mask shape. Our main contributions are as follows:

- To the best of our knowledge, PowerPaint stands as a groundbreaking inpainting model, surpassing existing approaches by simultaneously achieving state-of-the-art performance across multiple inpainting tasks.
- We demonstrate the versatility of the task prompts in PowerPaint, showcasing their capability to serve as negative prompts for effective object removal, as well as enabling controllable shape-guided object inpainting through prompt interpolation.
- Our extensive evaluation encompasses both quantitative and qualitative assessments, providing comprehensive evidence to substantiate the effectiveness of PowerPaint in addressing a wide range of inpainting challenges.

2. Related Work

2.1. Image Inpainting

Image inpainting is an effective editing tool that enables users to mask and edit specific regions in an image [3–5, 7]. With the significant progress of deep learning, some works have gained remarkable achievements by leveraging generative adversarial networks (GAN) [10, 35, 36]. These approaches often randomly mask any regions in an image and are optimized to recover the masked region [20, 21, 35]. Through such optimization, these models are able to fill in the region with content that is coherent with the image context. However, these approaches can not infer new objects from the image context and fail to synthesize novel contents.

Recent advancements have been greatly promoted by text-to-image diffusion models [8, 13, 24, 27]. Specifically, SD-Inpainting [25] and ControlNet-Inpainting [37] are both built upon the large-scale pre-trained text-to-image model, *i.e.*, Stable Diffusion [25]. They fine-tune a pre-trained T2I model for inpainting with random masks as the inpainting masks and image captions as the text prompt. Despite some good results, these models often suffer from text misalignment and fail to synthesize objects that align with the text prompt. Smartbrush and Imagen Editor propose to address this issue by using paired object-description data for training [31, 32]. However, these models tend to assume that there are always objects in the missing regions, losing the ability to perform context-aware image inpainting. We highlight that, through learning different task prompts for different tasks, PowerPaint significantly improves the text and context alignment, leading to state-of-the-art results in both context-aware

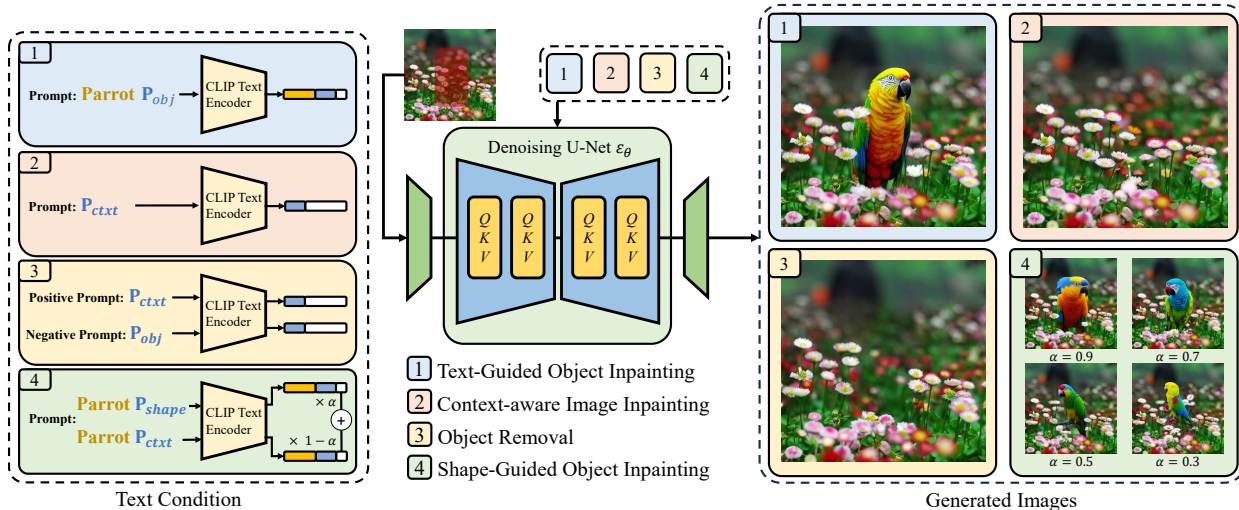


Figure 2. **The overview of PowerPaint.** PowerPaint fine-tunes a text-to-image model with two task prompts, i.e., \mathbf{P}_{obj} and \mathbf{P}_{ctxt} , for text-guided object inpainting and context-aware image inpainting, respectively. Specifically, \mathbf{P}_{obj} can be used as a negative prompt with classifier-free guidance sampling for effective object removal. We further introduce \mathbf{P}_{shape} for shape-guided object inpainting, which can be further extended by prompt interpolation with \mathbf{P}_{ctxt} to control how closely the generated objects should align with the mask shape.

image inpainting and text-guided object inpainting.

2.2. Adapting Text-to-Image Models

Text-to-image generative models have achieved remarkable advances in recent years, showcasing their ability to generate realistic and diverse images based on natural language descriptions [24, 25, 27]. These models have opened up a wide array of applications that leverage their generative power [9, 14, 26]. One notable example is DreamBooth, which fine-tunes the model to associate specific visual concepts with textual cues, enabling users to create personalized images from text [26]. Textual Inversion demonstrates that a single word vector can encode a unique and novel visual concept, which can then be inverted to generate an image [9]. Additionally, Kumari et al. [14] propose a method to simultaneously learn multiple visual concepts and seamlessly blend them with existing ones by optimizing a few parameters. Instead of object-specific prompts, we propose the utilization of task-specific prompts to guide text-to-image models for various tasks. Through fine-tuning both the textual embeddings and model parameters, we establish a robust alignment between the task prompts and the desired outputs.

3. PowerPaint

To enhance a pre-trained text-to-image diffusion model for high-quality and versatile inpainting, we introduce three learnable task prompts: \mathbf{P}_{obj} , \mathbf{P}_{ctxt} , and \mathbf{P}_{shape} , as shown in Figure 2. By incorporating these task prompts along with tailored training strategies, PowerPaint is able to deliver outstanding performance in various inpainting tasks, such as

text-guided object inpainting, context-aware image inpainting, object removal, and shape-guided object inpainting.

3.1. Preliminary

PowerPaint is built upon the well-trained text-to-image diffusion model, *i.e.*, Stable Diffusion, which comprises both forward and reverse processes [25]. In the forward process, a noise is added to a clean image x_0 in a closed form,

$$x_t = \sqrt{\bar{\alpha}_t}x_0 + \sqrt{1 - \bar{\alpha}_t}\epsilon, \epsilon \sim \mathcal{N}(0, I), \quad (1)$$

where x_t is the noisy image at timestep t , and $\bar{\alpha}_t$ denotes the corresponding noise level. In the reverse process, a neural network parameterized by θ , denoted as ϵ_θ , is optimized to predict the added noise ϵ_t . This enables the generation of images by denoising step by step from Gaussian noise. A classical diffusion model is typically optimized by:

$$\mathcal{L} = \mathbb{E}_{x_0, t, \epsilon_t} \|\epsilon_t - \epsilon_\theta(x_t, t)\|_2^2. \quad (2)$$

To fine-tune Stable Diffusion for inpainting, PowerPaint begins by extending the first convolutional layer of the denoising network ϵ_θ with five additional channels specifically designed for the masked image $x_0 \odot (1 - m)$ and masks m . The input to PowerPaint consists of the concatenation of the noisy latent, masked image, and masks, denoted as x'_t . Additionally, the denoising process can be guided by additional information such as text y . The model is optimized using the following objective function:

$$\mathcal{L} = \mathbb{E}_{x_0, m, t, y, \epsilon_t} \|\epsilon_t - \epsilon_\theta(x'_t, \tau_\theta(y), t)\|_2^2, \quad (3)$$

where $\tau_\theta(\cdot)$ is the CLIP text encoder. Importantly, PowerPaint extends the text condition by incorporating learnable task prompts, which serve as guidance for the model to accomplish diverse inpainting tasks.

3.2. Learning with Task Prompts

Context-aware image inpainting and text-guided object inpainting are prominent applications in the field of inpainting, each demanding distinct training strategies for optimal results [21, 25, 35]. To seamlessly integrate these two distinct objectives into a unified model, we propose the use of two learnable task prompts dedicated to each task. These task prompts serve as guidance for the model, enabling it to effectively accomplish the desired inpainting targets.

Context-aware Image Inpainting. Context-aware image inpainting aims to fill in the user-specified regions with content that seamlessly integrates with the surrounding image context. Previous studies have shown that training models with random masks and optimizing them to reconstruct the original image yields the best results [19, 21, 35]. This training strategy effectively encourages the model to attend to the image context and fill in coherent content. To achieve this, we introduce a learnable task prompt, denoted as \mathbf{P}_{ctx} , which serves as the text condition during training. Additionally, we randomly mask the image region as part of the training process. During model fine-tuning, \mathbf{P}_{ctx} is optimized by:

$$p_{\text{ctx}} = \arg \min_p \mathbb{E}_{x_0, m, t, p, \epsilon_t} \|\epsilon_t - \epsilon_\theta(x'_t, \tau_\theta(p), t)\|_2^2, \quad (4)$$

where p is randomly initialized as an array of tokens and then used as input to the text encoder. This formulation enables users to seamlessly fill in regions with coherent content without explicitly specifying the desired content.

Text-guided Object Inpainting. Synthesizing novel objects that cannot be inferred solely from the image context often requires additional guidance provided by text prompts. Successful approaches in this area have leveraged paired object-caption data during training, allowing the model to generate objects that align with the provided text prompts [25, 31, 32]. To achieve this, we introduce a learnable task prompt, denoted as \mathbf{P}_{obj} , which serves as the task hint for text-guided object inpainting. Specifically, \mathbf{P}_{obj} shares similar optimization functions as Equation (4), but with two differences. First, for a given training image, we utilize the detected object’s bounding box as the inpainting mask. Second, we append \mathbf{P}_{obj} as a suffix to the text description of the masked region, which serves as the input to the text encoder. After training, our model effectively learns to inpaint images based on either the given context or text descriptions.

Object Removal. PowerPaint can be used for object removal, where users can use a mask to cover the entire object and condition the model on the task prompt \mathbf{P}_{ctx} to fill

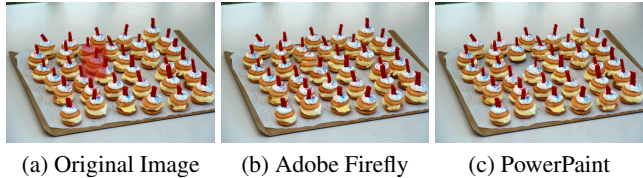


Figure 3. To remove objects from crowded image context, the state-of-the-art solution (Adobe Firefly [1]) tends to copy from the context, while PowerPaint successfully erases the objects.

in coherent content. However, it becomes more challenging when attempting to remove objects in crowded contexts. As shown in Figure 3, even state-of-the-art solutions like Adobe Firefly [1], while generating visually pleasing content, tend to synthesize objects within the masked region. We suspect that the inherent network structure, which includes attention layers, leads to the model paying excessive attention to the context. This makes it easier for the model to ‘copy’ information from the crowded context and ‘paste’ it into the masked region, resulting in object synthesis instead of removal.

Fortunately, \mathbf{P}_{ctx} and \mathbf{P}_{obj} can be combined with a powerful classifier-free guidance sampling strategy [12] to achieve effective object removal. This strategy transforms the denoising process into the following form:

$$\tilde{\epsilon}_\theta = w \cdot \epsilon_\theta(x'_t, \tau_\theta(p_{\text{ctx}}), t) + (1 - w) \cdot \epsilon_\theta(x'_t, \tau_\theta(p_{\text{obj}}), t), \quad (5)$$

where \mathbf{P}_{ctx} is considered a positive prompt, while \mathbf{P}_{obj} is considered a negative prompt, and w is the guidance scale. The classifier-free guidance strategy works by decreasing the likelihood conditioned on the negative prompt and increasing the likelihood conditioned on the positive prompt for the sample. With this design, the likelihood of generating objects can be effectively decreased to achieve object removal, as demonstrated in Figure 3. This outcome indicates that the task prompts in PowerPaint have successfully captured the patterns associated with different inpainting tasks.

Controllable Shape Guided Object Inpainting. In this part, we explore shape-guided object inpainting, where the generated object aligns well with the given mask shape. To achieve this, we introduce a third task prompt, denoted as $\mathbf{P}_{\text{shape}}$, which is trained using precise object segmentation masks and object descriptions, following previous works [32]. However, we have noticed that relying solely on $\mathbf{P}_{\text{shape}}$ can lead the model to overfit the mask shape while disregarding the overall shape of the object. For instance, when provided with the prompt “a cat” and a square mask, the model may generate cat textures within the square mask without considering the realistic shape of a cat.

To address the above limitation and offer users a more reasonable and controllable shape-guided object inpainting, we propose task prompt interpolation. We start by randomly dilating the object segmentation masks using a convolutional-

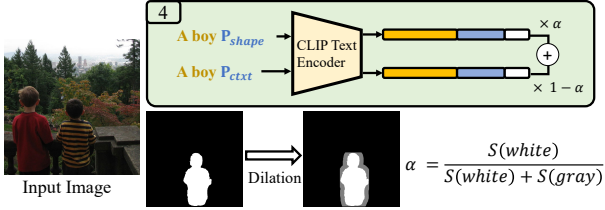


Figure 4. The values of mask and unmasked ratio are used as the weights of task prompt interpolation.

based dilation operation D , which is denoted as,

$$m' = D(m, k, it) \quad (6)$$

where k denotes the kernel size, and it denotes the iteration of dilation. This generates a set of masks with varying fitting degrees to the object shape. For each training mask, we calculate the area ratio, α , representing the fitting degree. A larger α indicates a closer fit to the mask shape, while a smaller α indicates a looser fit. To perform prompt interpolation, we append P_{shape} and P_{ctxt} as suffixes to the text description y and separately input them into the CLIP Text Encoder. This yields two text embeddings. By linearly interpolating these embeddings based on the value of α , as shown in Figure 4, we obtain the final text embedding, which is denoted as:

$$\tau'_\theta = \alpha \cdot \tau_\theta(y, p_{ctxt}) + (1 - \alpha) \cdot \tau_\theta(y, p_{shape}). \quad (7)$$

After training, users can adjust the value of α to control the fitting degree of the generated objects to the mask shape.

3.3. Implementation Details

We fine-tune the task prompt parameters in the embedding layer of the CLIP text encoder and the U-net based on the Stable Diffusion v1.5 model. PowerPaint was trained for 25K iterations on 8 A100 GPUs with a batch size of 1024 and a learning rate of $1e-5$. We use the semantic segmentation subset of OpenImage v6[15] as the main dataset for multi-task prompt tuning. In addition, following Smartbrush [32], we use segmentation labels and BLIP captions[16] as local text descriptions. Simultaneously, we treat the text-to-image generation task as a special case of inpainting (mask everything), and use the image/text pairs from the LAION-Aesthetics v2 5+[28] for training. The main task and the text-to-image generation task have probabilities of 80% and 20%, respectively, in the training phase.

4. Experiments

4.1. Experimental Setup

Baselines. To verify the superior performance of PowerPaint in various inpainting tasks, we select the most recent, competitive, and available inpainting approaches for fair

comparisons. We list these approaches with their abbreviations and brief introductions below:

- **LaMa** [29] is built upon a generative adversarial network [10] and achieves state-of-the-art in large mask inpainting.
- **LDM-Inpainting** [25] is finetuned from a text-to-image latent diffusion model for inpainting without text prompt.
- **Blended Diffusion** [2] achieves text-guided inpainting by leveraging a language-image model (CLIP) [23].
- **Stable Diffusion** [25] achieves text-guided inpainting by blending the unmasked latent in each denoising step.
- **SD-Inpainting** [25] fine-tuned Stable Diffusion with random masks and image caption for inpainting.
- **ControlNet-Inpainting** [37] controls Stable Diffusion for inpainting by a condition encoder that encodes masks.

Evaluation Benchmarks. To make fair comparisons with SOTA approaches, we adopt the most commonly-used datasets for inpainting following previous works [25, 29, 32]. First, we evaluate text-guided object inpainting on **OpenImages** [15] and **MSCOCO** [18]. We randomly sample 10k images from the test set of OpenImages and MSCOCO, and then we sample two kinds of masks for each testing image, *i.e.*, bounding box masks that contain the object of interest and the exact object layout segmentation masks, following Xie *et al.* [32]. We use the class label of the object as the text prompt for testing. Second, we evaluate context-aware image inpainting on **Places2** [39]. We sample 10k images from the test set of Places2 and generate random masks as inpainting masks following Rombach *et al.* [25, 29]. In this setting, there is no text prompt provided for evaluation and the inpainting model should fill in regions according to image contexts. Finally, we evaluate the performance of image outpainting without text prompt on 10K images from **Flickr-Scenery**, which are the most representative and natural use-cases of outpainting, following Cheng *et al.* [6, 30, 34].

Evaluation Metrics. We use five numeric metrics for different inpainting tasks, *i.e.*, Fréchet Inception Distance (FID) [11], Local-FID [32], CLIP Score [23], LPIPS [38], and aesthetic score [28], following common settings [6, 25, 29, 31, 32]. Specifically, we use FID and Local-FID for global and local image visual quality. The CLIP Score is used in text-guided object inpainting to evaluate the alignment of generated visual content with the text prompt. Since context-aware image inpainting aims at recovering the randomly masked regions according to image contexts, we use the original image as ground truths and use LPIPS to evaluate the reconstruction performance. Finally, we introduce an aesthetic score for outpainting, which aims to evaluate the extended image content for pleasing scenery content.

4.2. Comparisons with State-of-the-Art

Quantitative Comparisons. We report quantitative evaluation on various inpainting benchmarks following previous

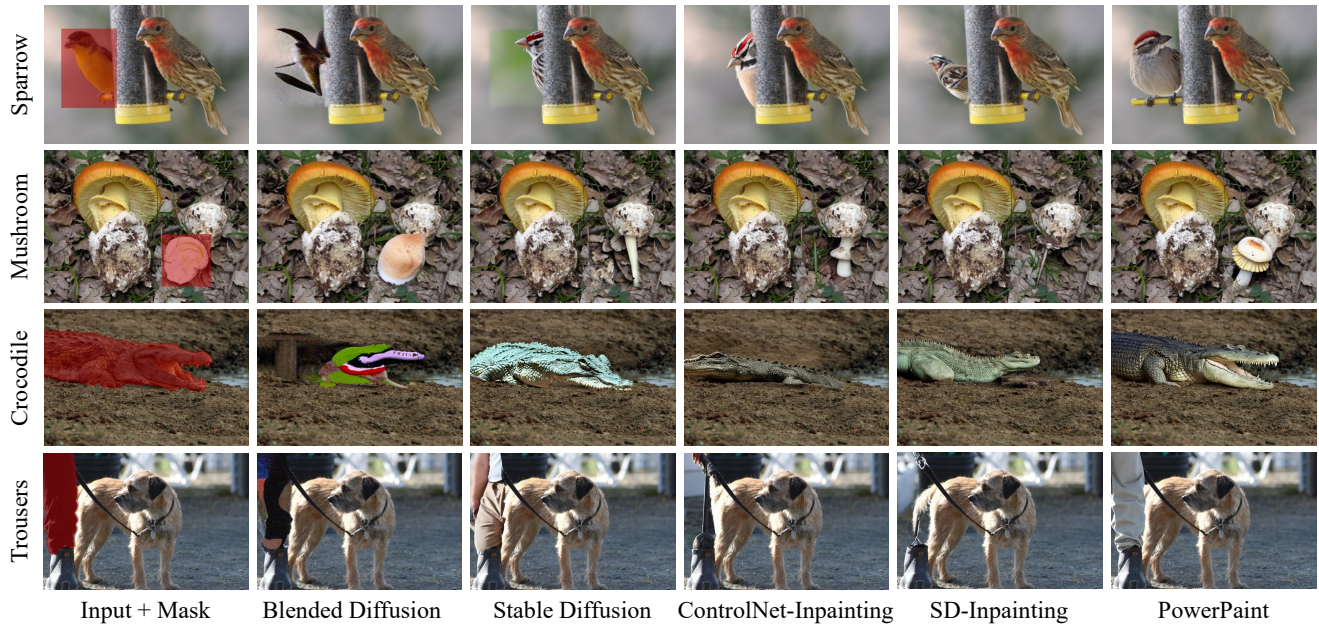


Figure 5. Compared with SOTA approaches, PowerPaint shows better text alignment and visual quality for text-guided object inpainting.

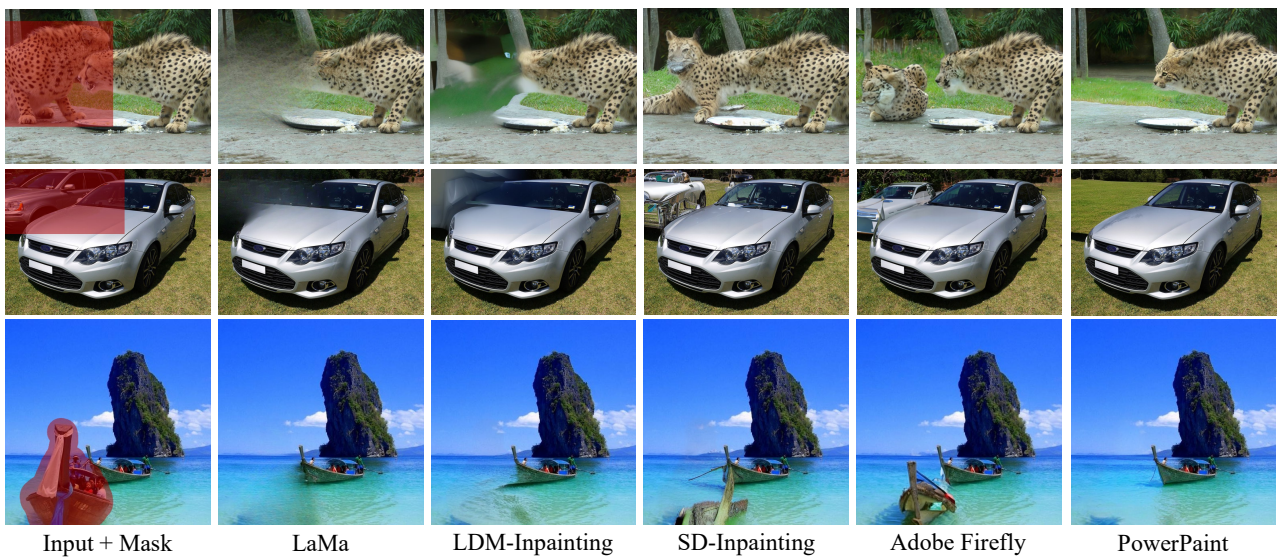


Figure 6. Compared with SOTA approaches, PowerPaint shows better context alignment for context-aware image inpainting.



Figure 7. Compared with SOTA approaches, PowerPaint shows more pleasing results for image outpainting with a large expand.

Table 1. Quantitative comparisons with state-of-the-art models for text-guided object inpainting with bounding box masks.

	OpenImages [15]			MSCOCO [18]		
	Local-FID↓	FID↓	CLIP Score↑	Local-FID↓	FID↓	CLIP Score↑
Blended Diffusion [2]	35.66	8.07	27.05	34.65	4.76	24.98
Stable Diffusion [25]	16.75	6.59	26.79	19.99	3.91	25.15
ControlNet-Inpainting [37]	14.74	5.66	26.87	16.84	3.32	25.04
SD-Inpainting [25]	12.71	4.76	26.66	13.67	2.77	24.70
PowerPaint	10.91	4.69	27.61	12.86	2.73	26.07

Table 2. Quantitative comparisons with state-of-the-art models for shape-guided object inpainting with object layout masks.

	OpenImages [15]			MSCOCO [18]		
	Local-FID↓	FID↓	CLIP Score↑	Local-FID↓	FID↓	CLIP Score↑
Blended Diffusion [2]	22.69	6.87	26.60	17.78	2.55	24.72
Stable Diffusion [25]	13.94	4.98	26.47	13.82	2.37	24.49
ControlNet-Inpainting [37]	11.96	4.54	26.45	11.60	2.17	24.39
SD-Inpainting [25]	10.73	3.93	26.31	10.61	1.98	24.29
PowerPaint	8.19	3.68	27.19	8.90	1.93	25.63

works [29, 32]. For text-guided object inpainting and shape-guided object inpainting, we use bounding box masks and object layout masks for testing on OpenImages [15] and MSCOCO [18], respectively. The results in Table 1 and Table 2 demonstrate that PowerPaint generates realistic and diverse images that satisfy both the text and shape constraints better than the baselines.

For context-aware image inpainting, we include text-free inpainting models, *i.e.*, LaMa [29] and LDM-Inpaint [25], and the second strongest inpainting model shown in Table 1 and 2, *i.e.*, SD-Inpainting for further comparison. The quantitative results shown in Table 3 demonstrate that PowerPaint guided by a task-specific prompt, outperforms the baseline in effectively filling missing regions while better matching the image context. To further substantiate this comparison, we prompt SD-Inpainting with a default text as ‘background’ and ‘scenery’, juxtaposed against PowerPaint augmented with P_{obj} as a negative prompt. We observed that P_{obj} , as a negative prompt, significantly suppresses the generation of random artifacts and retains a coherent background in harmony with the image context, thereby markedly enhancing the fill quality and achieving optimal performance. Lastly, considering that the goal of image outpainting is to extend the image with content that is both aesthetically pleasing and coherent, we employed FID and aesthetic scores for its quantitative evaluation. As indicated in Table 4, our model demonstrates superior image and aesthetic quality compared to the baseline models.

Qualitative Comparisons. The qualitative comparison in Figure 13, 6 and 7 show that our model has achieved state-of-the-art performance in text-guided object inpainting, context-aware image inpainting, and outpainting. For text-guided object inpainting, existing models often fail to synthesize objects that are faithful to the text prompt. For example, in

Table 3. Quantitative comparisons for context-aware image inpainting with random masks on Places2 [39].

	40-50% masked		All samples	
	FID ↓	LPIPS ↓	FID ↓	LPIPS ↓
LaMa [29]	21.07	0.2133	3.48	0.1193
LDM-Inpaint [25]	21.42	0.2317	3.42	0.1325
SD-Inpainting [25]	19.73	0.2322	3.03	0.1312
PowerPaint w/o neg	19.17	0.2301	2.89	0.1308
SD-Inpainting(‘background’)	19.21	0.2290	2.82	0.1293
SD-Inpainting(‘scenery’)	18.93	0.2312	2.84	0.1306
PowerPaint w/ neg	17.96	0.2226	2.60	0.1264

Table 4. Quantitative results for outpainting on Flickr-Scenery [6].

	FID ↓	Aesthetic Score ↑
LaMa [29]	16.63	5.01
LDM-Inpainting [25]	11.00	5.10
SD-Inpainting [25]	58.38	5.22
SD-Inpainting(‘background’)	24.67	5.25
SD-Inpainting(‘scenery’)	13.31	5.30
PowerPaint	10.13	5.32

the fourth case, ControlNet-Inpainting and SD-Inpainting are hard to generate trousers in the region and can only fill the region with backgrounds. PowerPaint is able to synthesize high-fidelity objects according to the text prompt with both bounding box masks and object layout masks. For context-aware image inpainting, our model outperforms both text-free and text-based inpainting models significantly. Taking the second case in Figure 6 as an example, LaMa tends to synthesize blurry results due to its limited generation capacity, while Adobe Firefly [1] tends to generate random objects in the region, which goes against the users’ intention. Similar conclusions can be found in outpainting. Our model can naturally extend the scenery image with pleasing content.

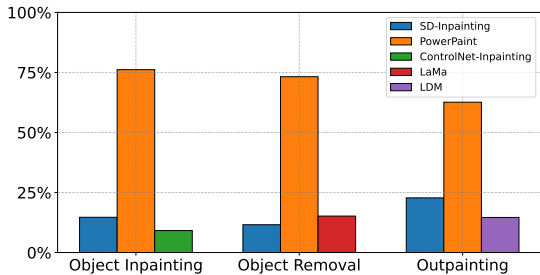


Figure 8. PowerPaint wins the first place in the user studies.



Figure 9. Object removal in comparison with Adobe Firefly [1].

User study. We conducted user studies for a more comprehensive comparison. Specifically, we deliver three groups of user studies for text-guided object inpainting, object removal, and outpainting, respectively. For each group, we randomly sample test images and show the inpainting results to volunteers anonymously. In each trial, we introduce different inpainting tasks to the volunteers and ask them to choose the most satisfying results per different targets. We have collected 2,200 valid votes and conclude the results in Figure 8. The results show that our model is chosen as the most satisfactory inpainting technique in all three tasks.

4.3. Analysis

We showcase the versatility of PowerPaint through task prompts, demonstrating its applications in object removal, controllable shape-guided object inpainting, and conducting an ablation study. Importantly, PowerPaint seamlessly integrates with ControlNet, allowing for extensive controllable inpainting under different conditions such as depth and pose. More results can be found in the appendix.

Object Removal. We find it challenging to remove objects from crowded image contexts for inpainting models based on diffusion model, which often copies context objects into regions due to the intrinsic network structure (*i.e.*, self-attention layers). We show in Figure 9 that, combined with classifier-free guidance strategy, our model uses \mathbf{P}_{obj} as a negative prompt so that it can prevent generating objects in regions for effective object removal.

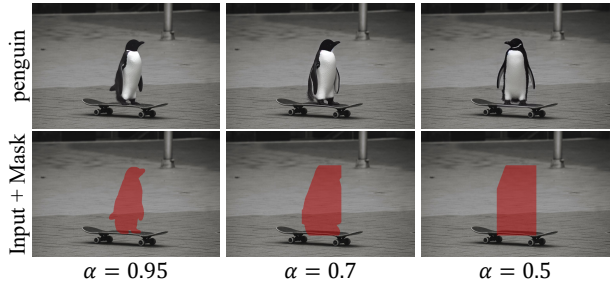


Figure 10. Application of shape-guided object inpainting.

Table 5. ablation study on text-guided object inpainting.

	Local-FID↓	FID ↓	CLIP Score↑
identifier	13.01	2.75	26.01
PowerPaint	12.86	2.73	26.07

Table 6. ablation study on context-aware image inpainting.

	40-50% masked		All samples	
	FID ↓	LPIPS↓	FID ↓	LPIPS↓
identifier w/o neg	19.91	0.2331	3.19	0.1319
PowerPaint w/o neg	19.17	0.2301	2.89	0.1308

Shape-Guided Object Inpainting. Given a mask, PowerPaint enables users to control the fitting degree to the mask shape by adjusting the interpolation of two leaned task prompts, *i.e.*, \mathbf{P}_{ctx} and \mathbf{P}_{shape} . Results in Figure 10 show that PowerPaint can synthesize high-fidelity results that are faithful to both the mask shape and text prompt.

Ablation Study. To verify the effectiveness of task prompt learning, we compare our model with the variant of tuning with unlearnable rare identifiers [26]. In this variant, we use different rare identifiers to denote different tasks with the same training strategies as PowerPaint. The quantitative comparison in Table 5 and 6 show that a learnable task prompt can be better compatible with the description and conditions (*i.e.*, masked images and masks) for different inpainting targets, leading to better results.

5. Limitations and Conclusions

We present PowerPaint as a groundbreaking inpainting model that outperforms existing approaches by achieving state-of-the-art performance across multiple inpainting tasks. Our method’s success is rooted in its utilization of task prompts and tailored optimal training strategies.

Our method does have two inherent limitations. Firstly, the synthesis quality can be constrained by the capabilities of the underlying text-to-image diffusion model. We plan to alleviate this limitation by extending our method to a more powerful text-to-image diffusion model, such as SDXL [22]. Secondly, in the case of shape-guided object inpainting, we have observed that achieving a fitting degree with extremely small values is challenging. This limitation arises from the sparse representation of instances where objects occupy ex-

tremely small regions during training. To overcome this, we are committed to investing additional effort in improving the training strategy for various inpainting targets, including those with challenging shapes and sizes.

We will make our models and codes publicly available. In this supplementary material, we show more qualitative comparisons with state-of-the-art approaches for various inpainting tasks and the results of combining PowerPaint with ControlNet for more controllable image inpainting.

A. More Qualitative Comparisons

We compare PowerPaint with several state-of-the-art methods for text-guided and shape-guided object inpainting, context-aware image inpainting, and outpainting. Specifically, the baselines for text-guided and shape-guided object inpainting are Blended Diffusion [2], Stable Diffusion [25], ControlNet-Inpainting [37], and SD-Inpainting [25]. The baselines for context-aware image inpainting and outpainting are LaMa [29], LDM-Inpainting [25], ControlNet-Inpainting, and SD-Inpainting. We show some qualitative results in the following figures.

Figure 11 and Figure 12 show some qualitative results of text-guided object inpainting. The input images have a masked region and a text description of the desired object to fill in the region. We can see that PowerPaint generates realistic and coherent objects that match the text descriptions and the input images. The baselines either fail to generate the correct objects, produce distorted or blurry objects, or introduce artifacts or inconsistencies in the inpainted images.

Figure 13 shows some qualitative results of shape-guided object inpainting. We can see that PowerPaint can generate realistic and diverse images that match the given shape masks. The baselines either fail to fill the missing regions, or generate images that do not conform to the shape masks. PowerPaint also maintains the coherence and harmony of the images better than the baselines.

Figure 14 shows some qualitative results of context-aware image inpainting. The input images have a masked region that covers a portion of the image. The goal is to fill in the region with realistic and coherent content that matches the context of the image. We can see that PowerPaint generates realistic and coherent content that matches the context of the image. The baselines either fail to generate realistic or coherent content, produce distorted or blurry content, or introduce artifacts or inconsistencies in the inpainted images.

Figure 15 shows some qualitative results of outpainting. The input images have a smaller size than the desired output size. The goal is to extend the image boundaries with realistic and coherent content that matches the context of the image. We can see that PowerPaint generates realistic and coherent content that matches the context of the image. The baselines either fail to generate realistic or coherent content, produce distorted or blurry content, or introduce artifacts or

inconsistencies in the outpainted images.

B. PowerPaint with ControlNet

We further evaluate the compatibility of PowerPaint with different ControlNets [37]. Specifically, users can directly insert ControlNet into PowerPaint, which enables taking additional conditions to guide the inpainting. We test four types of ControlNets for different conditions: canny edge , depth , hed boundary , and human pose . The results are shown in Figures 16 to 19.

We can see that PowerPaint can perform well with different ControlNets, and generate images that are of good quality and match the conditions of the ControlNet outputs. It shows that PowerPaint can directly use the existing ControlNet to achieve rich conditional control.

References

- [1] Adobe Firefly, 2023. <https://firefly.adobe.com/>. 4, 7, 8
- [2] Omri Avrahami, Dani Lischinski, and Ohad Fried. Blended diffusion for text-driven editing of natural images. In *Proceedings of the IEEE/CVF Conference on Computer Vision and Pattern Recognition*, pages 18208–18218, 2022. 5, 7, 9, 10, 11, 12
- [3] Connelly Barnes, Eli Shechtman, Adam Finkelstein, and Dan B Goldman. Patchmatch: A randomized correspondence algorithm for structural image editing. *TOG*, 28(3):24:1–24:11, 2009. 1, 2
- [4] Marcelo Bertalmio, Guillermo Sapiro, Vincent Caselles, and Coloma Ballester. Image inpainting. In *SIGGRAPH*, pages 417–424, 2000. 1
- [5] Marcelo Bertalmio, Luminita Vese, Guillermo Sapiro, and Stanley Osher. Simultaneous structure and texture image inpainting. *TIP*, 12(8):882–889, 2003. 2
- [6] Yen-Chi Cheng, Chieh Hubert Lin, Hsin-Ying Lee, Jian Ren, Sergey Tulyakov, and Ming-Hsuan Yang. Inout: Diverse image outpainting via gan inversion. In *Proceedings of the IEEE/CVF Conference on Computer Vision and Pattern Recognition*, pages 11431–11440, 2022. 5, 7
- [7] Antonio Criminisi, Patrick Pérez, and Kentaro Toyama. Region filling and object removal by exemplar-based image inpainting. *TIP*, 13(9):1200–1212, 2004. 2
- [8] Prafulla Dhariwal and Alexander Nichol. Diffusion models beat gans on image synthesis. *Advances in neural information processing systems*, 34:8780–8794, 2021. 2
- [9] Rinon Gal, Yuval Alaluf, Yuval Atzmon, Or Patashnik, Amit H Bermano, Gal Chechik, and Daniel Cohen-Or. An image is worth one word: Personalizing text-to-image generation using textual inversion. *arXiv preprint arXiv:2208.01618*, 2022. 3
- [10] Ian Goodfellow, Jean Pouget-Abadie, Mehdi Mirza, Bing Xu, David Warde-Farley, Sherjil Ozair, Aaron Courville, and

<https://huggingface.co/llyasviel/sd-controlnet-canny>

<https://huggingface.co/llyasviel/sd-controlnet-depth>

<https://huggingface.co/llyasviel/sd-controlnet-hed>

<https://huggingface.co/llyasviel/sd-controlnet-openpose>

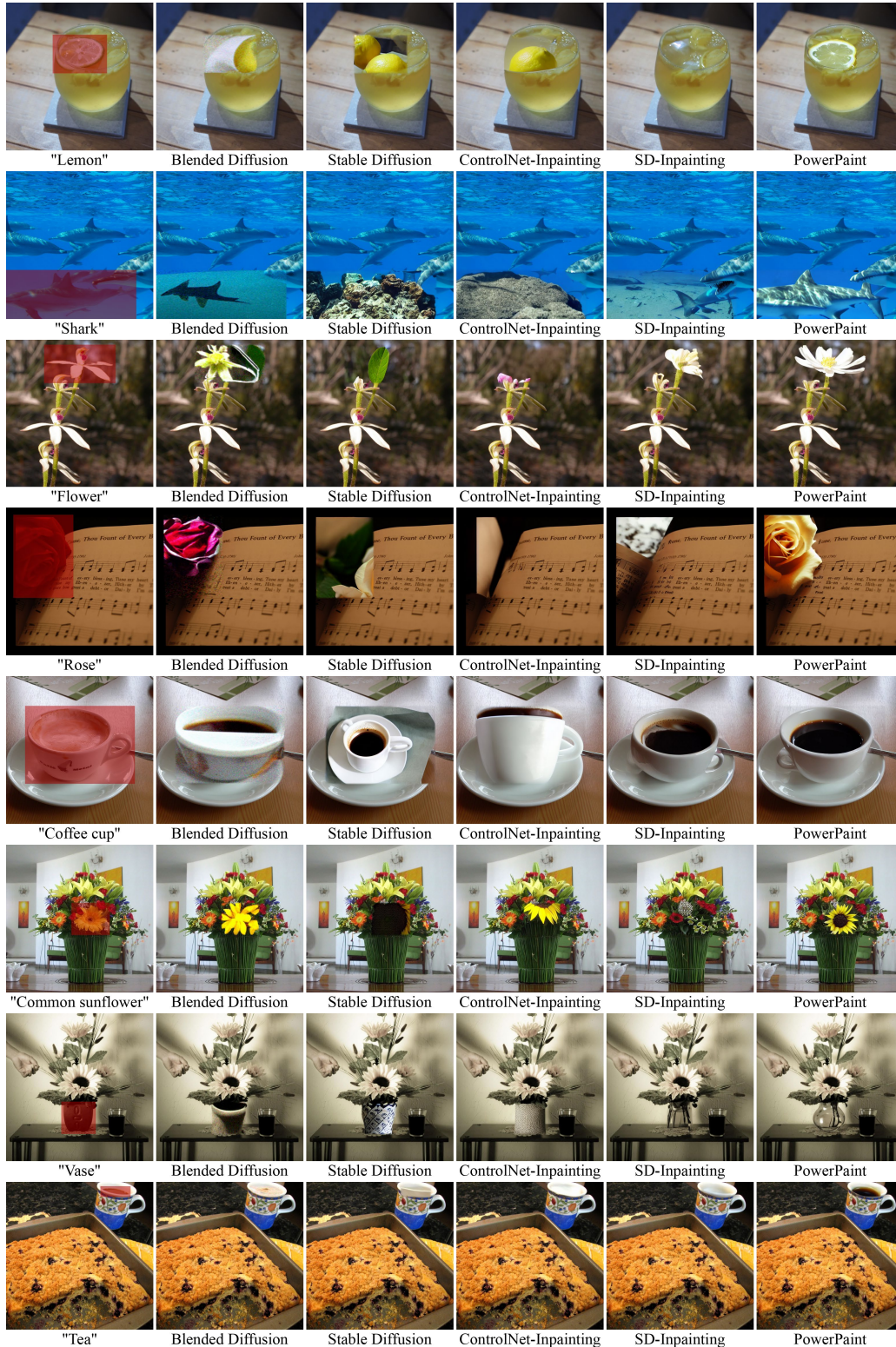


Figure 11. For text-guided object inpainting, we compare PowerPaint with Blended Diffusion [2], Stable Diffusion [25], ControlNet-Inpainting [37] and SD-Inpainting [25]. PowerPaint shows much better text alignment and visual quality. [Best viewed with zoom-in in color]

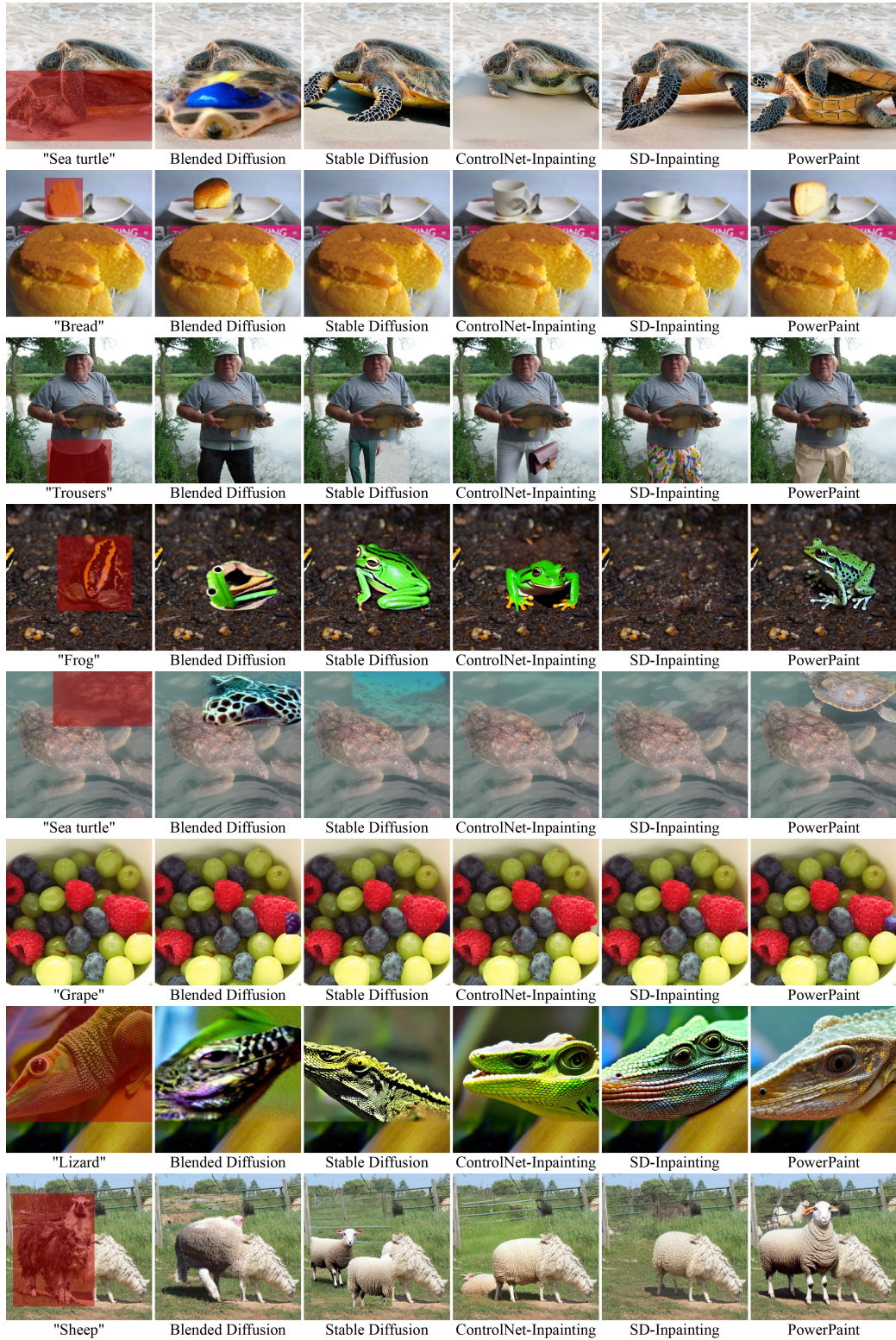


Figure 12. For text-guided object inpainting, we compare PowerPaint with Blended Diffusion [2], Stable Diffusion [25], ControlNet-Inpainting [37] and SD-Inpainting [25]. PowerPaint shows much better text alignment and visual quality. [Best viewed with zoom-in in color]

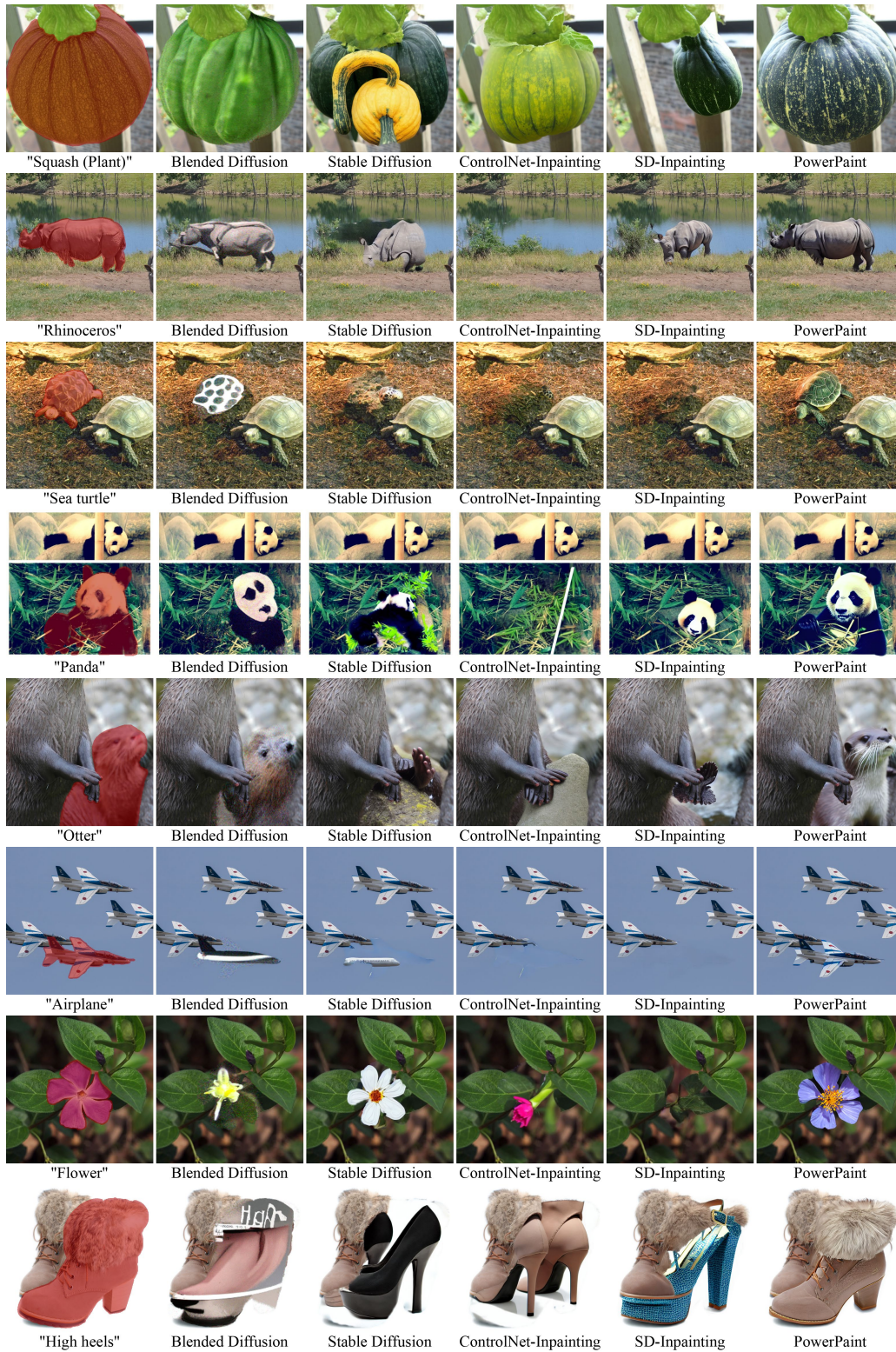


Figure 13. For shape-guided object inpainting, we use exact object layout masks as inpainting masks. We compare PowerPaint with Blended Diffusion [2], Stable Diffusion [25], ControlNet-Inpainting [37] and SD-Inpainting [25]. PowerPaint shows better text alignment and shape alignment. [Best viewed with zoom-in in color]

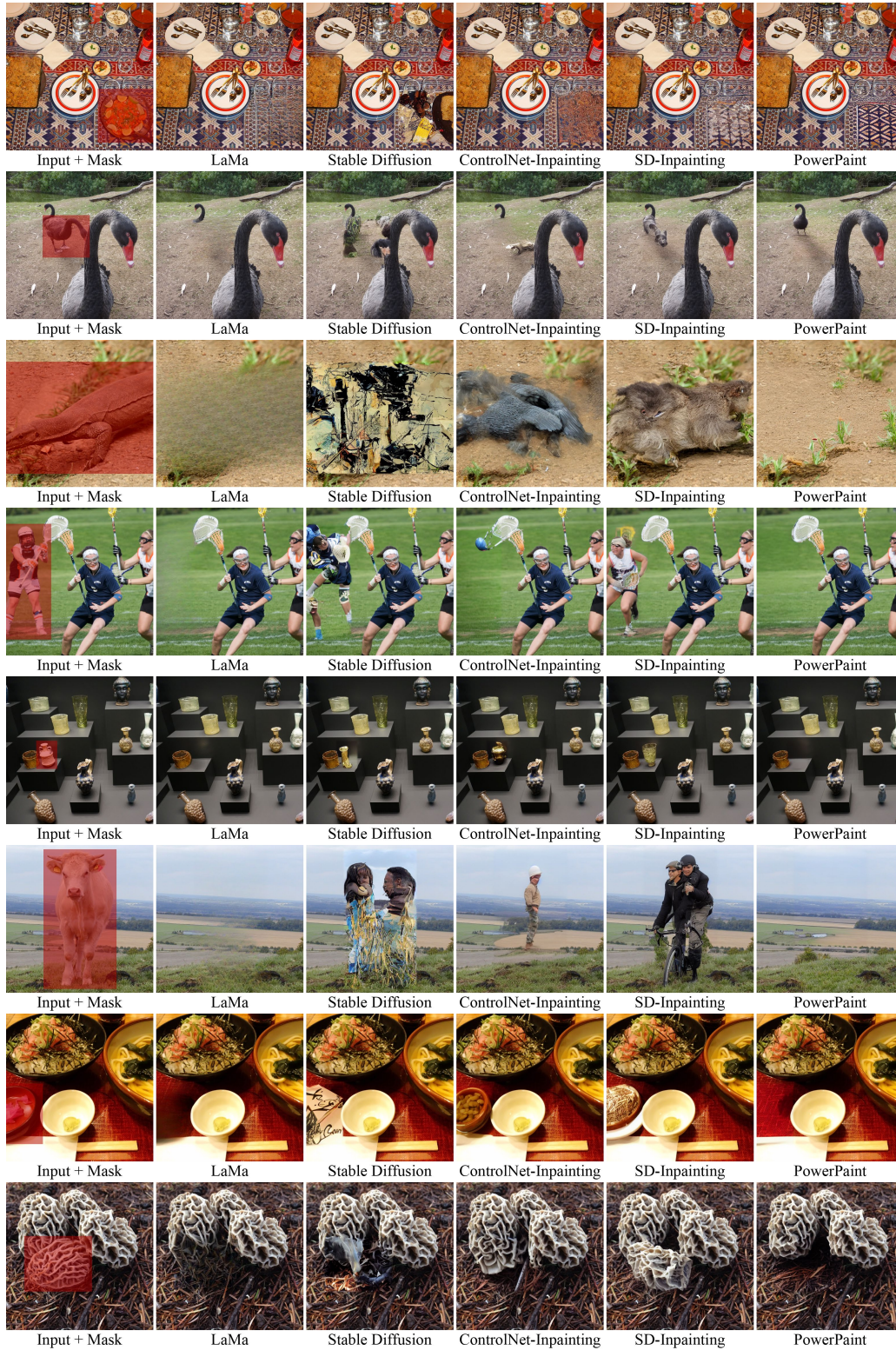


Figure 14. For context-aware image inpainting, users do not need input text prompts for inpainting. We compare PowerPaint with LaMa [29], Stable Diffusion [25], ControlNet-Inpainting [37] and SD-Inpainting [25]. PowerPaint is able to synthesize high-quality and context-aware results. [Best viewed with zoom-in in color]

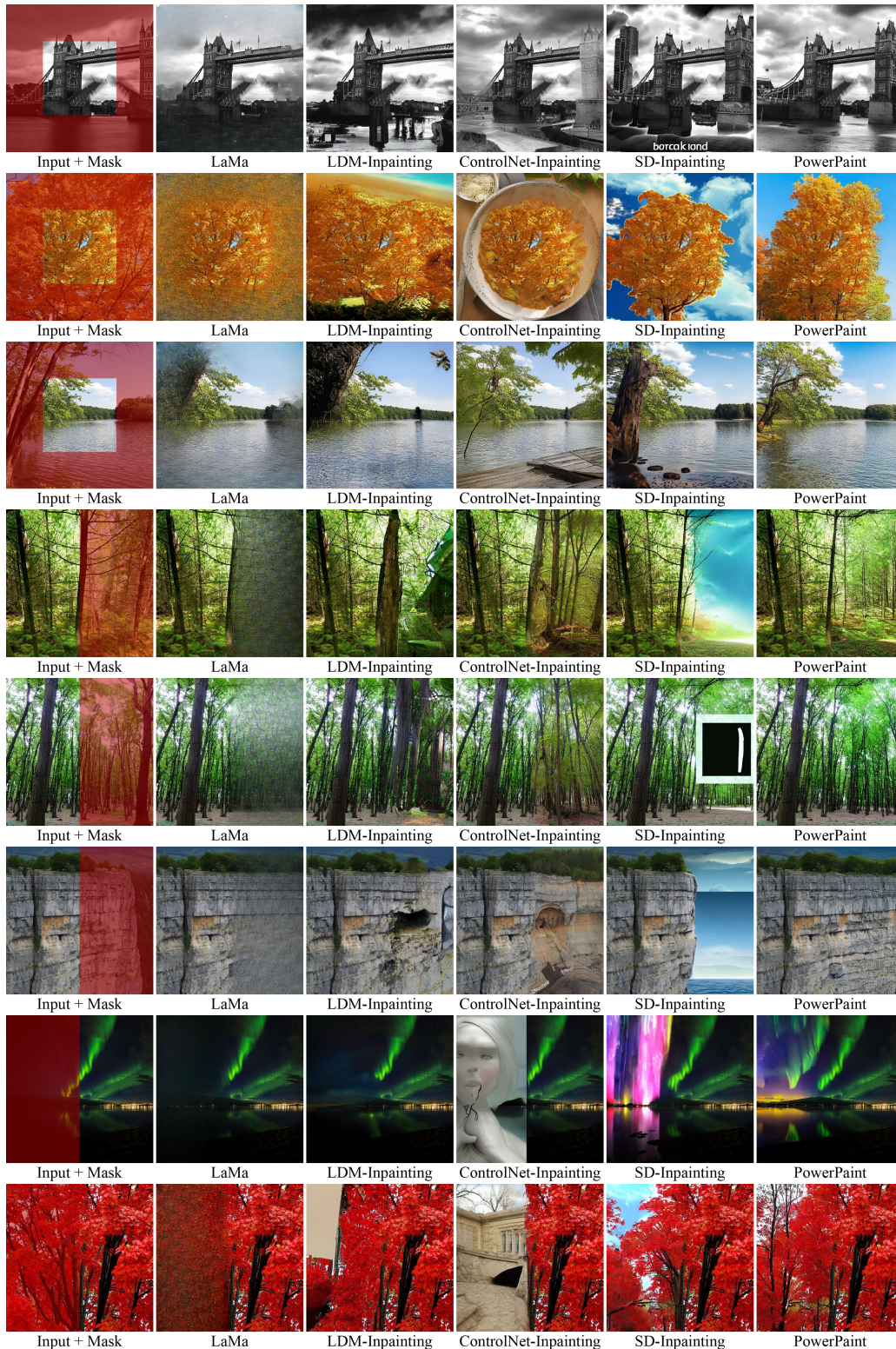


Figure 15. For image inpainting, we compare PowerPaint with LaMa [29], LDM-Inpainting [25], ControlNet-Inpainting [37] and SD-Inpainting [25] with various inpainting masks. PowerPaint is able to expand the input image with much more pleasing results. [Best viewed with zoom-in in color]

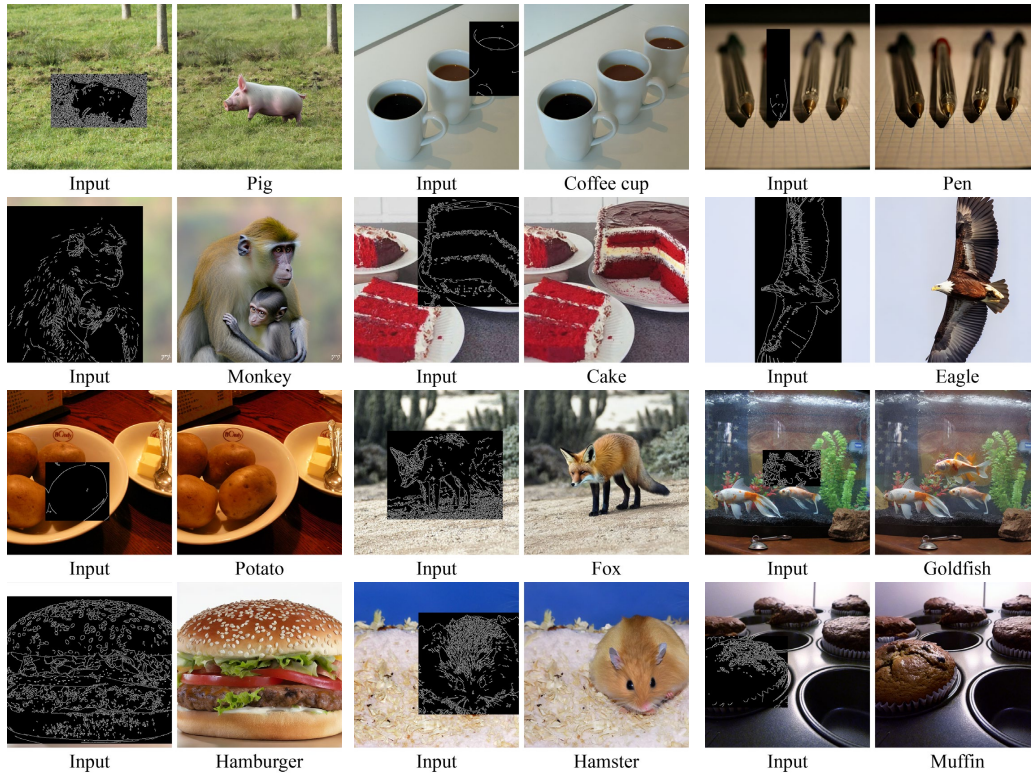


Figure 16. Qualitative Evaluation of PowerPaint with the ControlNet conditioned on canny.

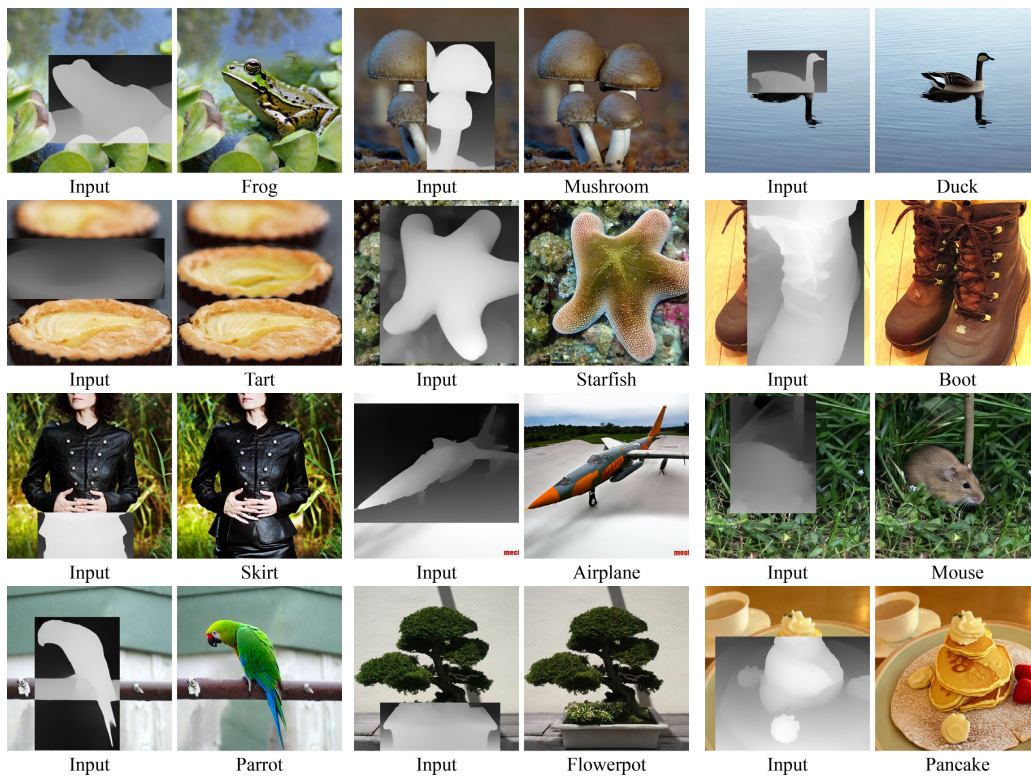


Figure 17. Qualitative Evaluation of PowerPaint with the ControlNet conditioned on depth.

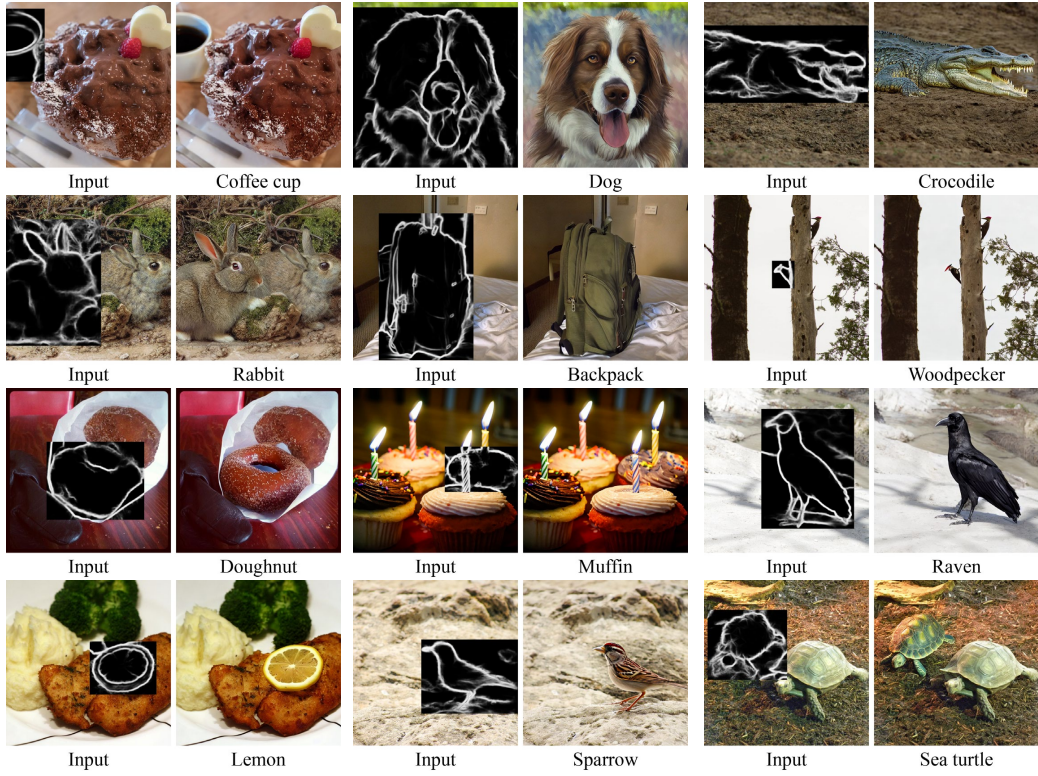


Figure 18. Qualitative Evaluation of PowerPaint with the ControlNet conditioned on hed.

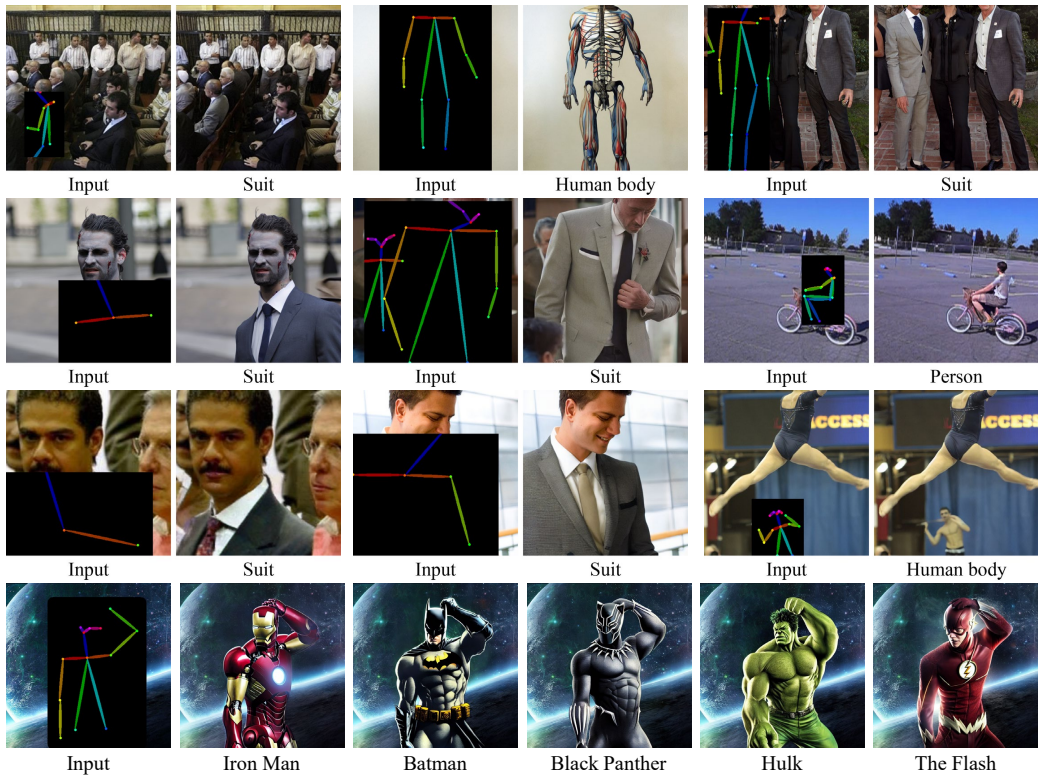


Figure 19. Qualitative Evaluation of PowerPaint with the ControlNet conditioned on pose.

- Yoshua Bengio. Generative adversarial nets. In *NeurIPS*, pages 2672–2680, 2014. 2, 5
- [11] Martin Heusel, Hubert Ramsauer, Thomas Unterthiner, Bernhard Nessler, and Sepp Hochreiter. Gans trained by a two time-scale update rule converge to a local nash equilibrium. *Advances in neural information processing systems*, 30, 2017. 5
- [12] Jonathan Ho and Tim Salimans. Classifier-free diffusion guidance. In *NeurIPS 2021 Workshop on Deep Generative Models and Downstream Applications*, 2021. 2, 4
- [13] Jonathan Ho, Ajay Jain, and Pieter Abbeel. Denoising diffusion probabilistic models. *Advances in neural information processing systems*, 33:6840–6851, 2020. 2
- [14] Nupur Kumari, Bingliang Zhang, Richard Zhang, Eli Shechtman, and Jun-Yan Zhu. Multi-concept customization of text-to-image diffusion. In *Proceedings of the IEEE/CVF Conference on Computer Vision and Pattern Recognition (CVPR)*, pages 1931–1941, 2023. 3
- [15] Alina Kuznetsova, Hassan Rom, Neil Alldrin, Jasper Uijlings, Ivan Krasin, Jordi Pont-Tuset, Shahab Kamali, Stefan Popov, Matteo Mallocci, Alexander Kolesnikov, Tom Duerig, and Vittorio Ferrari. The open images dataset v4: Unified image classification, object detection, and visual relationship detection at scale. *International Journal of Computer Vision*, 128(7):1956–1981, 2020. 5, 7
- [16] Junnan Li, Dongxu Li, Silvio Savarese, and Steven Hoi. Blip-2: Bootstrapping language-image pre-training with frozen image encoders and large language models, 2023. 5
- [17] Yijun Li, Sifei Liu, Jimei Yang, and Ming-Hsuan Yang. Generative face completion. In *CVPR*, pages 3911–3919, 2017. 1
- [18] Tsung-Yi Lin, Michael Maire, Serge Belongie, James Hays, Pietro Perona, Deva Ramanan, Piotr Dollár, and C Lawrence Zitnick. Microsoft coco: Common objects in context. In *Computer Vision—ECCV 2014: 13th European Conference, Zurich, Switzerland, September 6–12, 2014, Proceedings, Part V 13*, pages 740–755. Springer, 2014. 5, 7
- [19] Andreas Lugmayr, Martin Danelljan, Andres Romero, Fisher Yu, Radu Timofte, and Luc Van Gool. Repaint: Inpainting using denoising diffusion probabilistic models. In *Proceedings of the IEEE/CVF Conference on Computer Vision and Pattern Recognition*, pages 11461–11471, 2022. 1, 2, 4
- [20] Kamyar Nazeri, Eric Ng, Tony Joseph, Faisal Qureshi, and Mehran Ebrahimi. Edgeconnect: Generative image inpainting with adversarial edge learning. In *ICCVW*, 2019. 2
- [21] Deepak Pathak, Philipp Krahenbuhl, Jeff Donahue, Trevor Darrell, and Alexei A Efros. Context encoders: Feature learning by inpainting. In *CVPR*, pages 2536–2544, 2016. 1, 2, 4
- [22] Dustin Podell, Zion English, Kyle Lacey, Andreas Blattmann, Tim Dockhorn, Jonas Müller, Joe Penna, and Robin Rombach. Sdxl: Improving latent diffusion models for high-resolution image synthesis. *arXiv preprint arXiv:2307.01952*, 2023. 8
- [23] Alec Radford, Jong Wook Kim, Chris Hallacy, Aditya Ramesh, Gabriel Goh, Sandhini Agarwal, Girish Sastry, Amanda Askell, Pamela Mishkin, Jack Clark, et al. Learning transferable visual models from natural language supervision. In *International conference on machine learning*, pages 8748–8763. PMLR, 2021. 5
- [24] Aditya Ramesh, Mikhail Pavlov, Gabriel Goh, Scott Gray, Chelsea Voss, Alec Radford, Mark Chen, and Ilya Sutskever. Zero-shot text-to-image generation. In *International Conference on Machine Learning*, pages 8821–8831. PMLR, 2021. 1, 2, 3
- [25] Robin Rombach, Andreas Blattmann, Dominik Lorenz, Patrick Esser, and Björn Ommer. High-resolution image synthesis with latent diffusion models. In *Proceedings of the IEEE/CVF conference on computer vision and pattern recognition*, pages 10684–10695, 2022. 1, 2, 3, 4, 5, 7, 9, 10, 11, 12, 13, 14
- [26] Nataniel Ruiz, Yuanzhen Li, Varun Jampani, Yael Pritch, Michael Rubinstein, and Kfir Aberman. Dreambooth: Fine tuning text-to-image diffusion models for subject-driven generation. In *Proceedings of the IEEE/CVF Conference on Computer Vision and Pattern Recognition*, pages 22500–22510, 2023. 3, 8
- [27] Chitwan Saharia, William Chan, Saurabh Saxena, Lala Li, Jay Whang, Emily L Denton, Kamyar Ghasemipour, Raphael Gontijo Lopes, Burcu Karagol Ayan, Tim Salimans, et al. Photorealistic text-to-image diffusion models with deep language understanding. *Advances in Neural Information Processing Systems*, 35:36479–36494, 2022. 1, 2, 3
- [28] Christoph Schuhmann, Romain Beaumont, Richard Vencu, Cade Gordon, Ross Wightman, Mehdi Cherti, Theo Coombes, Aarush Katta, Clayton Mullis, Mitchell Wortsman, et al. Laion-5b: An open large-scale dataset for training next generation image-text models. *Advances in Neural Information Processing Systems*, 35:25278–25294, 2022. 5
- [29] Roman Suvorov, Elizaveta Logacheva, Anton Mashikhin, Anastasia Remizova, Arsenii Ashukha, Aleksei Silvestrov, Naejin Kong, Harshith Goka, Kiwoong Park, and Victor Lempitsky. Resolution-robust large mask inpainting with fourier convolutions. In *Proceedings of the IEEE/CVF winter conference on applications of computer vision*, pages 2149–2159, 2022. 1, 2, 5, 7, 9, 13, 14
- [30] Piotr Teterwak, Aaron Sarna, Dilip Krishnan, Aaron Maschinot, David Belanger, Ce Liu, and William T Freeman. Boundless: Generative adversarial networks for image extension. In *Proceedings of the IEEE/CVF International Conference on Computer Vision*, pages 10521–10530, 2019. 5
- [31] Su Wang, Chitwan Saharia, Ceslee Montgomery, Jordi Pont-Tuset, Shai Noy, Stefano Pellegrini, Yasumasa Onoe, Sarah Laszlo, David J Fleet, Radu Soricut, et al. Imagen editor and editbench: Advancing and evaluating text-guided image inpainting. In *Proceedings of the IEEE/CVF Conference on Computer Vision and Pattern Recognition*, pages 18359–18369, 2023. 2, 4, 5
- [32] Shaoan Xie, Zhifei Zhang, Zhe Lin, Tobias Hinz, and Kun Zhang. Smartbrush: Text and shape guided object inpainting with diffusion model. In *Proceedings of the IEEE/CVF Conference on Computer Vision and Pattern Recognition*, pages 22428–22437, 2023. 2, 4, 5, 7
- [33] Shiyuan Yang, Xiaodong Chen, and Jing Liao. Uni-paint: A unified framework for multimodal image inpainting with

- pretrained diffusion model. In *Proceedings of the 31st ACM International Conference on Multimedia*, pages 3190–3199, 2023. [2](#)
- [34] Zongxin Yang, Jian Dong, Ping Liu, Yi Yang, and Shuicheng Yan. Very long natural scenery image prediction by out-painting. In *Proceedings of the IEEE/CVF International Conference on Computer Vision*, pages 10561–10570, 2019. [5](#)
- [35] Jiahui Yu, Zhe Lin, Jimei Yang, Xiaohui Shen, Xin Lu, and Thomas S Huang. Generative image inpainting with contextual attention. In *CVPR*, pages 5505–5514, 2018. [1](#), [2](#), [4](#)
- [36] Jiahui Yu, Zhe Lin, Jimei Yang, Xiaohui Shen, Xin Lu, and Thomas S Huang. Free-form image inpainting with gated convolution. In *ICCV*, pages 4471–4480, 2019. [2](#)
- [37] Lvmin Zhang, Anyi Rao, and Maneesh Agrawala. Adding conditional control to text-to-image diffusion models. In *Proceedings of the IEEE/CVF International Conference on Computer Vision*, pages 3836–3847, 2023. [1](#), [2](#), [5](#), [7](#), [9](#), [10](#), [11](#), [12](#), [13](#), [14](#)
- [38] Richard Zhang, Phillip Isola, Alexei A Efros, Eli Shechtman, and Oliver Wang. The unreasonable effectiveness of deep features as a perceptual metric. In *CVPR*, pages 586–595, 2018. [5](#)
- [39] Bolei Zhou, Agata Lapedriza, Aditya Khosla, Aude Oliva, and Antonio Torralba. Places: A 10 million image database for scene recognition. *IEEE transactions on pattern analysis and machine intelligence*, 40(6):1452–1464, 2017. [5](#), [7](#)